Contents lists available at ScienceDirect

CIRP Annals
Manufacturing Technology
Journal homepage: www.elsevier.com/locate/cirp

A new hybrid Minimum Quantity Lubrication system for machining difficult-to-cut materials

Alborz Shokrani[a]*, Joseph Betts[a]

[a] University of Bath, Bath, BA2 7AY, United Kingdom

Submitted by T. H. C. Childs (1), Leeds, United Kingdom

A newly designed and manufactured hybrid MQL system is reported. Vegetable oil and tungsten disulphide suspension are mixed in an additively-manufactured nozzle and delivered through pressurised air as a coolant/lubricant spray. Cooling capability of the system is improved. Lubrication and the impact on machinability is assessed in high speed milling Ti6Al4V. Tool life and cutting forces with the new system are compared to those with air and with flood cooling and with commercial MQL. Over the reported practical range of cutting speeds, tool life is more than 2 times longer than with the commercial system and from 4 to 11 times longer than with air cooling.

Cooling; lubrication; machining.

1. Introduction

Since their introduction, cutting fluids have been an indispensable part of material cutting systems, specifically for difficult-to-cut materials such as titanium and nickel alloys [1]. They reduce heat generation and improve heat dissipation from the cutting zone and enhance machinability. Minimum Quantity Lubrication (MQL) effectively reduces cutting fluid consumption in machining [2] and the use of vegetable-based oil as an alternative to petroleum or synthetic lubricants enhances their sustainability. Nevertheless, penetrability and cooling capability have remained an issue in MQL machining, especially in high speed machining and specifically in milling operations.

Various micro and nanoparticles have been added to MQL fluids to enhance their cooling capabilities. Alumina [3] and diamond [4] nanoparticles have been shown to enhance the thermal conductivity of lubricants in MQL. Solid lubricants such as MoS_2 and graphite have been used to enhance lubricity. Refractory metal dichalcogenides such as WS_2 and TaS_2 have higher thermal stability than MoS_2 and graphite.

Despite being recognised as a solid lubricant, there is little study of WS_2 impact in machining and the studies are limited to WS_2 soft coatings [5]. Being a soft coating, WS_2 wears quickly, minimally impacting tool life. An alternative is introducing WS_2 through the MQL stream, effectively to deliver WS_2 throughout the machining operation. Paturi et al. [6] dispersed WS_2 in emulsifier oil based cutting fluid in turning Inconel 718. However, this study is limited to surface roughness analysis.

The addition of micro and nanoparticles to a fluid impacts its flow and rheological behaviour [7]. This paper reports computational fluid mechanics (CFD) and convective heat transfer studies, as well as tool life testing for a range of traditional and new MQL fluid delivery methods, to develop both improved operation of and insights into MQL.

The delivery methods are by flood cooling, with a commercial MQL process (CMQL), and with a newly designed MQL nozzle spraying both rapeseed oil alone (Oil) and a mixture of rapeseed oil and a WS_2–rapeseed oil suspension (OWS) as well as pressurised air alone (Air).

The particular condition investigated is high speed milling of Ti6Al4V with a coated solid carbide end mill. With nozzles placed in optimum positions, OWS increases heat transfer from the tool by ≈ 10% relative to other MQL systems and by 75% relative to Air; and tool life by more than 2 times relative to CMQL and by 4 to 11 times relative to Air, depending on cutting speed.

2. Methodology

2.1. Experimental setup and new MQL system

Figures 1a (new nozzle) and b (commercial nozzles) illustrate schematic views of the experimental setup. A 5 flute, 12 mm diameter solid carbide end mill with TiSiN coating [8] is used to machine straight tracks on a 50 × 50 × 150 mm block of Ti-6Al-4V. The nozzles, directed at the cutting zone, are inclined vertically at the tool helix angle and have a variable inclination α horizontally (Fig. 1c). The new nozzle (Fig. 1d), designed and made by stereolithography 3D printing, has a 1 mm diameter exit orifice and three separate inlets, for compressed air, rapeseed oil and WS_2-rapeseed oil suspension at 1% concentration, and two mixing chambers. The WS_2 is made up of lamellar sheets characterised by hexagonal crystal structure of S–W–S.

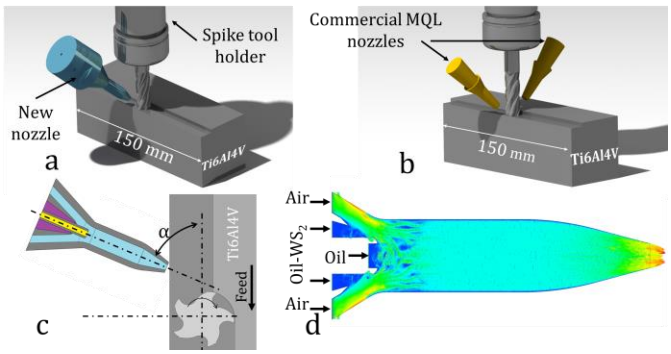

Figure 1. Experimental setup, with a) the new and b) commercial nozzles. c) gives the nozzle orientation α and d) shows detail of the new nozzle.

Rapeseed oil and WS_2–rapeseed oil suspension are delivered to the nozzle at 50 ml/hr each, whilst an air pressure of 5 bar is used. The flow rate of the air is measured to be 6.1 m^3/h. These are the maximum values that the pumps can take. For the conventional nozzles, with 2.5 mm diameter orifices, 100 ml/hr oil and 6 bar pressure are used based on previous studies; and for flood cooling, a 7% solution of emulsion in water is applied.

2.2. Nozzle development and positioning

The spray generation from the nozzle has been investigated both by using a two stage axisymmetric 2D CFD simulation, created in Ansys Fluent, and physically. In a further simulation, interaction of the spray with the rotating end milling tool has been explored to determine the optimum α positioning of the nozzle.

Volume of fluid (VoF) method [9] was used in the first stage to simulate fluid mixing within the nozzle. The flow rates for oil and WS_2-oil, with their measured viscosities (rapeseed oil: 0.059 Pas; WS_2–rapeseed oil: 0.7 Pas) as well as the air supply pressure as input, lead to a prediction of velocity profile at the nozzle exit. The second stage takes the output from the first stage as an input to predict the pressure and velocity field away from the nozzle, assuming a steady state condition. The CFD simulation results have been validated experimentally by pressure field measurement throughout the jet by means of a static pitot tube and differential manometer. The jet velocity profile has been computed using Bernoulli's principle based on differential pressure measurements as presented in 3.1. In addition, droplets from the new nozzle have been collected on a silicon wafer and examined microscopically to determine their compositions, diameters and diameter distribution.

The spray-tool interaction has been simulated via a 2.5D time transient model of the jet, rotating tool and work, with Fig. 1c geometry, with minimum time step 10^{-20} s and k-ε turbulence model. The tool and its mesh, of 10 µm size around the cutting zone, rotate at 3980 rpm to give the surface speed of 150 m/min. Pressure staggering options with second order scheme were used for solving the model. The optimum position of the nozzle was judged by maximising the wall jet flow and pressure at the cutting zone and in the space between the cutting tool and the workpiece.

2.3. Heat transfer

The cooling capabilities of the different arrangements have been measured directly. The rotating milling tool was induction heated to 350 °C, then cooled by the different methods: Air, Oil, CMQL and OWS. Tool temperature reduction with time was measured by both a FLIR 6000 scientific series infrared thermal camera and by two pyrometers. All were calibrated individually over the temperature range using k type thermocouples with 0.1 s response time. Tests were conducted at three peripheral speeds of the tool, namely 120, 150 and 200 m/min. Flood cooling could not be investigated since the flood coolant obscured the tool.

Cooling rates were converted to heat transfer coefficients, based on flow assumptions in [10], modelling heat transfer by Newton's law of cooling with the lumped capacitance method and checking the Biot number to ensure validity of the analysis.

Tests were conducted with a range of nozzle orientations relative to the rotating tool. Maximum heat transfer provided another means than by CFD to optimise the orientation. The orientation of the conventional nozzle was chosen in this way; that of the new nozzle was found to agree with the CFD analysis.

In all cases, nozzles were 25 mm from the tool, as they were in the actual machining tests.

2.4. Machining tests

In addition to the details in Section 2.1, the tool has axial and radial rake angles of 14° and 12° with a 3 µm thick TiSiN coating. The Ti6Al4V workpiece material has average hardness of 348±12 HV. All blocks were cut from a single plate to minimise variation in material properties.

Cutting speeds of 150 and 200 m/min were used, at a feed rate of 0.03 mm/tooth with 3 mm axial and 4 mm radial depth of cut. The machining experiments were performed on a vertical CNC machine, with all five different cooling/lubrication methods namely, Air, Flood, CMQL, Oil and OWS.

The power consumption of the machine tool was monitored continuously at 1 Hz. The power consumed for cutting is obtained by subtracting the power consumption in air cutting. Torque may be obtained by dividing power by the spindle speed.

The bending moment of the tool assembly was measured at 2.5 kHz using a Spike smart tool holder [11]. Radial force on the tool may be estimated by dividing the moment by the tool assembly overhang length (≈ 100 mm).

Tool flank wear was measured intermittently using a digital microscope, with a photographic record made. Tool life was taken as a maximum flank wear of 300 µm.

Experiments were at least duplicated for repeatability.

3. Results

3.1 Nozzle development and positioning

Figure 2 shows the simulated jet velocity contours, with experimental measurements added as the solid lines.

At 25 mm from the nozzle, the CFD analysis indicates a centre velocity of 286 m/s while the experimental value is 291 m/s. The diameter of the jet at 25 mm is approximately 4 mm. Velocity and diameter vary only slowly with distance from the nozzle at this distance which justifies not taking distance from the nozzle as a variable in optimizing the nozzle's positioning.

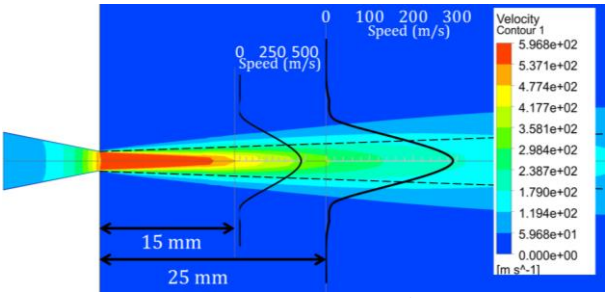

Figure 2. CFD and experimental velocity profile outside the new nozzle.

Droplets collected from the nozzle in OWS condition are shown in Fig. 3a. Droplets containing WS_2 are significantly larger than the oil droplets (Fig. 3b), showing the impact of solid suspension on atomisation of the oil. The average droplet diameter is 9 µm with a median of 7 µm (Fig. 3c).

Predicted jet/tool/work interactions are shown in Fig. 4. The interaction of the jet with the tool and workpiece depends on the nozzle orientation and geometry of the interaction. The geometry changes periodically with rotation of the tool. Entrainment of the jet into the cutting zone requires a driving local pressure to develop, commonly associated with stagnation of the flow at entry. It can be hindered by vortex formation or by shearing of the jet due to tool rotation, causing it to bend away from the cut. Even when a line of sight from the jet to the cutting zone opens up, fluid will not penetrate the cut if the appropriate pressure is not developed.

Figures 4a-c show three circumstances near to the α = 54° jet orientation that is optimum according to the Section 2.2 criterion. The tools are near to, but not all at, effective entrainment angular positions. In a) vortex formation blocks entrainment, in b) there is line-of-sight but little entrainment. Only for c) does a strong entrainment occur. One tooth in c) is marked by a red dot and d) shows it 1/5th of a revolution advanced. The flow is almost identical, confirming its rapid oscillation. Figure 3 e and f show very different flows at jet orientations far from optimum.

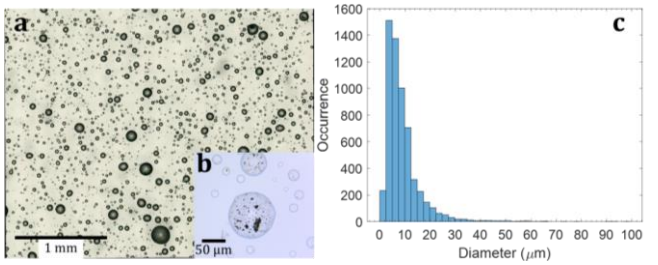

Figure 3. a) Droplet image with b) detail inset and c) diameter distribution.

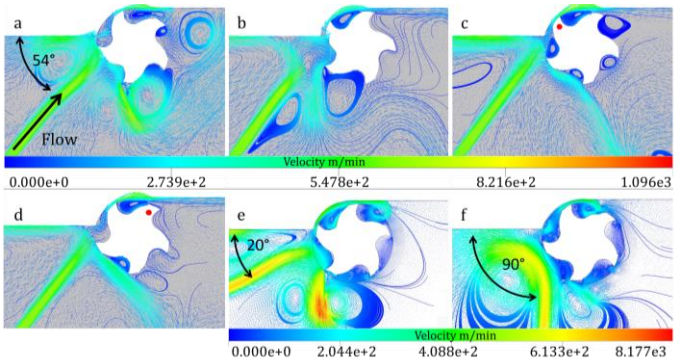

Figure 4. CFD velocity profile of fluid flow across a rotating end mill at the cutting zone (a-d) at optimum orientation and different time steps and (e-f) at a single time step but at non-optimum orientations α of 20° and 90°.

3.2. Heat transfer

The tool temperature was recorded under different conditions and the heat transfer coefficients calculated from the cooling tests with the new nozzle as shown in Fig. 5 a and b, respectively, for the optimum nozzle positioning. Air has least cooling capacity, as might be expected, followed by CMQL and Oil, with OWS performing best. For the new nozzle, optimum position is α = 54° as also concluded in Section 3.1, with a useful range ±5°, due to the small dimension of the jet. For CMQL the front nozzle (Fig. 1b) was optimized at α = 54° as well. The back nozzle was not studied. Its orientation was left at the standard value of 90°.

3.3. Machining tests

Figure 6a-c shows wear progression at the cutting speed of 150 m/min through all three measures of power consumption, bending moment and wear itself. Tool wear alone for the 200 m/min condition is shown in Fig. 6d and the wear is, as expected, far more rapid than at 150 m/min. The tool life at 200 m/min is 4, 6.5, 8, 11 and 17 mins respectively for Air, Flood, CMQL, Oil and OWS. The equivalent values at 150 m/min are 11, 14.5, 46 and 95 mins. The OWS test at 150 m/min was stopped after 120 min with only 150 µm of tool wear, limited by material availability.

At 150 m/min, the tools fail when the power and bending moment reach ≈ 480 W and 50 Nm. At zero time (and wear), the power is higher with Air and Flood cooling than with any MQL cases but bending moments are the same for all. It suggests a larger cutting force for Oil and Flood, i.e. a better lubrication and lower friction with MQL. The subsequent different wear rates among the MQL cases may be attributed to the different cooling effects.

Figure 7 shows tool wear images from the end of 150 m/min tests. In Air and CMQL, welding of the chips on the rake face is dominant. With flood cooling, crater wear occurs with chipping of the cutting edge. Flank wear increases along the cutting edge towards the depth of cut with Oil. Least wear is clear with OWS.

The rapid wear growth seen in Fig. 6 near the end of life is associated with failure of the tool coating. This is followed by adhesion of titanium on the exposed substrate. These end of test wear observations may not represent steady wear in all cases.

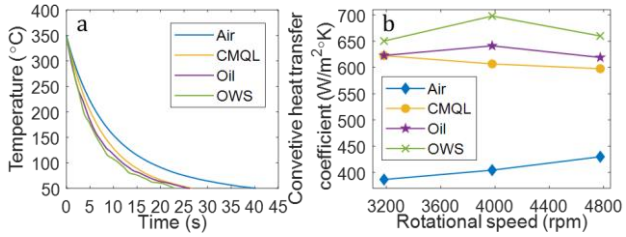

Figure 5. a) Temperature vs time at 3979 rpm (150 m/min) b) Convective heat transfer coefficient at different rotational speeds.

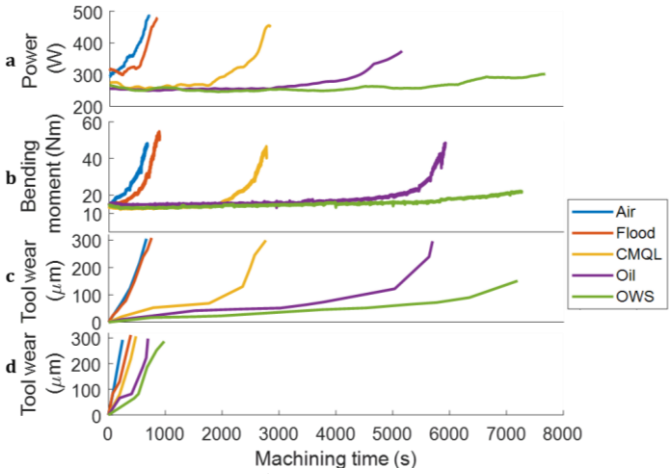

Figure 6. Increase with time of a) machining power, b) bending moment and c) tool wear at a cutting speed 150 m/min; (d) tool wear at 200 m/min.

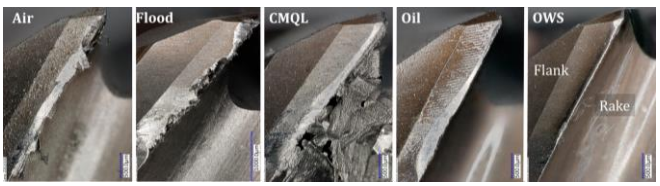

Figure 7. End of test tool wear images from the 150 m/min cutting condition.

4. Discussion

The tool life tests (Fig. 6) clearly demonstrate the superior performance of the newly designed nozzle in which, two separate fluids are mixed to form a spray both of oil droplets and of droplets containing WS_2 additive. Using this method results in longer tool life compared with the same nozzle spraying only the oil, demonstrating the impact of WS_2 additive. The new nozzle with just the single component spray also performs better than a commercial nozzle with the same oil, indicating the superior performance of the new nozzle design and highlighting the importance of the jet flow as well as its composition.

The analysis also confirms the difficulty of fluid penetration in milling. The heat transfer coefficients recorded in Fig. 5b are at best 700 W/m^2K, while values of 2500 W/m^2K are known in turning with flood cooling [12], yet tool life with all MQL tests greatly exceeded life from flood cooling. Through spindle lubrication was not considered in this study which will be investigated in future works.

Materials reasons for the superior performance of OWS are complex. Originally (Section 1), the WS_2 was added to the oil as a thermally stable lubricant. Minimal reduction in power consumption (Fig. 6) with unworn tools indicates limited impact of WS_2 on friction at the start of the machining experiments. The impact becomes more significant when the substrate is exposed and therefore, any lubricating action must be on worn clearance faces. The mechanism is therefore a combination of improved heat removal and minimised heat generation when using OWS.

The WS_2 additive however, creates a better heat transfer (Fig. 5b). On the other hand, Oil gives a longer tool life than CMQL despite Oil and CMQL having almost the same heat transfer and both using the same rapeseed oil. The main material difference between Oil and CMQL is a larger droplet size in CMQL whilst fine droplet size has been identified as beneficial in previous works [13]. But in OWS, the WS_2 is encased in larger droplets (Fig. 3).

A potential limitation with the heat transfer tests is the maximum applied temperature of 350 °C. It was chosen as being at the limit of liquid lubricants [14] and maybe representing the local temperature in milling. However, the temperature reduces during the heat transfer test while a steady temperature is held during cutting. It is indeed likely that the temperature stability of WS_2 up to 730 °C [5] is important in the cutting condition. A unifying explanation of the OWS superior cooling performance is that the combination of fine droplets (without WS_2) for heat transfer and larger droplets for delivering WS_2, most likely to the clearance face, are important. The WS_2 additive can reduce friction on the clearance face and prevent flank wear whilst minimising friction induced heat at the cutting zone.

Turning to the fluid and thermal elements of this paper, the agreement on optimum nozzle orientation from both heat transfer experiments and CFD simulation importantly shows that CFD is a valid optimization tool. When machining complex geometries, with complex tool paths, at least radial depth of cut changes, and changes can be even more extreme with 5-axis operations. The use of CFD to support optimization in varying conditions, and eventually to support active nozzle positioning, is a promising but long-term development from this work.

More immediately and generally applicable is the observation (Fig. 6) that wear is accompanied by increase in bending moment as also found by Kollment et al. [15]. The possibility of using bending moment to monitor tool condition and end of tool life is clear, though deciding at what stage to stop a process must depend on linking surface integrity to the tool wear.

5. Conclusions

This paper combines four elements to enhance practice and understanding of MQL milling of difficult-to-machine Ti6Al4V. These are i) the introduction of a new MQL delivery nozzle that mixes two fluids into a jet (in this case rapeseed oil and rapeseed oil-WS_2 suspension), ii) its use that increases tool life compared to four other delivery methods and, iii) CFD simulation and, iv) heat transfer measurement to optimize the set up.

The new system achieves a cooling heat transfer near to 700 W/m^2K at optimum set up and an increase in tool life of ≈ 1.5× compared to the next best MQL delivery system and between 3× and 11× compared to Air or Flood cooling, depending on cutting speed. Results for 150 and 200 m/min are reported.

CFD simulation shows the complexity of interaction between the coolant/lubricant jet and the rotating tool and workpiece in conditions of optimum heat transfer. The turbulence and formation of vortices affect the flow and its direction towards the cutting zone which becomes periodic over time.

Acknowledgement

This work has been supported by grants EP/S017615/1 and EP/S513738/1 from UK EPSRC. We wish to thank Professor Childs, Leeds University, for help in the paper's preparation.

References

[1] Klocke, F., Eisenblätter, G., 1997, Dry Cutting, CIRP Annals - Manufacturing Technology 46/2:519-526.

[2] Weinert, K., Inasaki, I., Sutherland, J.W., Wakabayashi, T., 2004, Dry Machining and Minimum Quantity Lubrication, CIRP Annals - Manufacturing Technology 53/2:511-537.

[3] Hegab, H., Kishawy, H.A. , Umer, U., Mohany, A., 2019, A model for machining with nano-additives based minimum quantity lubrication, The International Journal of Advanced Manufacturing Technology 102/5:2013-2028.

[4] Nam, J.S., Lee, P.-H., Lee, S.W., 2011, Experimental characterization of micro-drilling process using nanofluid minimum quantity lubrication, International Journal of Machine Tools and Manufacture 51/7:649-652.

[5] Kustas, F.M., Fehrehnbacher, L.L., Komanduri, R., 1997, Nanocoatings on Cutting Tools For Dry Machining, CIRP Annals - Manufacturing Technology 46/1:39-42.

[6] Paturi, U.M.R., Maddu, Y.R., Maruri, R.R., Narala, S.K.R., 2016, Measurement and Analysis of Surface Roughness in WS2 Solid Lubricant Assisted Minimum Quantity Lubrication (MQL) Turning of Inconel 718, Procedia CIRP 40/138-143.

[7] Peker, S.M., Helvaci, Ş.Ş., *Non-Newtonian Behavior of Solid–Liquid Suspensions*, in *Solid-Liquid Two Phase Flow*, S.M. Peker, et al., Editors. 2008, Elsevier: Amsterdam. p. 71-166.

[8] IonBond. *Hardcut - TiSiN multilayer coating*. 2020; Available from: https://www.ionbond.com/coating-services/cutting-tools/hardcut/.

[9] Nakayama, Y., *Chapter 15 - Computational Fluid Dynamics*, in *Introduction to Fluid Mechanics (Second Edition)*, Y. Nakayama, Editor. 2018, Butterworth-Heinemann. p. 293-327.

[10] Gradeck, M., Ouattara, J.A., Rémy, B., Maillet, D., 2012, Solution of an inverse problem in the Hankel space – Infrared thermography applied to estimation of a transient cooling flux, Experimental Thermal and Fluid Science 36/56-64.

[11] Pro-micron. *Spike smart tool holder*. 2020; Available from: https://www.pro-micron.de/spike/.

[12] Kops, L., Arenson, M., 1999, Determination of Convective Cooling Conditions in Turning, CIRP Annals 48/1:47-52.

[13] Kumari, N., Bahadur, V., Hodes, Salamon, M.T., Kolodner, P., Lyons, A., Garimella, S.V., 2010, Analysis of evaporating mist flow for enhanced convective heat transfer, International Journal of Heat and Mass Transfer 53/15:3346-3356.

[14] Zhu, S., Cheng, J., Qiao, Z., Yang, J., 2019, High temperature solid-lubricating materials: A review, Tribology International 133/206-223.

[15] Kollment, W., Leary, P.O., Ritt, R., Kl¨unsner, T., 2017, *Force based tool wear detection using Shannon entropy and phase plane*. in *2017 IEEE International Instrumentation and Measurement Technology Conference (I2MTC)*.